



# Journal of Applied Sciences

ISSN 1812-5654

**science**  
alert

**ANSI***net*  
an open access publisher  
<http://ansinet.com>

## Combined Photocatalytic and Fenton Oxidation of Methyl Orange Dye using Iron Exchanged Titanium Pillared Montmorillonite

<sup>1</sup>I. Fatimah, <sup>2</sup>P.R. Shukla and <sup>3</sup>F. Kooli

<sup>1</sup>Department of Chemistry, Islamic University of Indonesia, Jl. Kaliurang Km 14, Besi, Yogyakarta, 55581, Indonesia

<sup>2</sup>Department of Chemical Engineering, Curtin University of Technology, Australia

<sup>3</sup>Department of Chemistry, Taibah University, P.O. Box 30002, Al-Madinah Al-Munawwarah, Saudi Arabia

**Abstract:** Methyl orange dye degradation was investigated under a combined photocatalytic and Fenton based oxidation in the presence of TiO<sub>2</sub> and Fe<sup>3+</sup> ion. A noble photocatalyst was developed to carry out the combined oxidation by incorporating TiO<sub>2</sub> and Fe<sup>3+</sup> ion on the natural clay support. The catalyst was characterized by several techniques such as XRD, BET, Diffuse Reflectance UV-Vis and XRF. The oxidation reaction of MeO using the developed catalyst follows the traditional Langmuir-Hinshelwood model. As a result, it was observed that the synergistic effect of Fe<sup>3+</sup> immobilization and titanium oxide photo-catalysis results in faster and more efficient degradation of the contaminant as shown by its higher rate compared to the use of TiO<sub>2</sub>-Pillared Montmorillonite. Efficiency of degradation depends on the concentration of H<sub>2</sub>O<sub>2</sub> and catalyst dosage and although there was Fe released from catalyst in its application, catalyst shows the reusable properties due to similar degradation rate of first and second utilization.

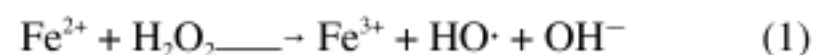
**Key words:** Photocatalyst, pillared clays, photo-fenton oxidation

### INTRODUCTION

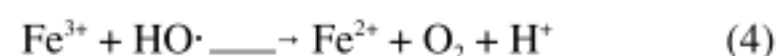
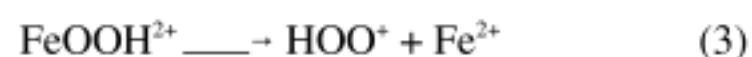
Bright and fabulous coloration, attractive outlook and ever changing fashion have revolutionised the textile industry which had been whole heartedly catering the current generation needs. In contrast to the front end production of beautiful fabrics, the backside discharge of waste water from many textile industries containing high concentration of dyes has raised a serious concern worldwide. The stability, non-biodegradability and toxicity pose a major threat to the surrounding aquatic system. The stability and non-biodegradability of the dye causes major problems in its treatment by primary and secondary treatment system and thus necessitating the need to employ the tertiary treatment methods.

There has been considerable research focus in last few decades on development of various techniques to treat dye waste water. Among various tertiary treatment methods, Advanced Oxidation Treatment (AOT) technique has been found to be promising to convert the dye present in waste water to harmless compounds. Advanced Oxidation Treatment techniques such as Fenton and Modified Fenton based treatment system, TiO<sub>2</sub> based photocatalysis, Ozonation,

Wet Air oxidation has been found to be quite effective in treatment of several organic contaminants (Bauer and Fallmann, 1997). Among all, modified Fenton based oxidation has been found to be efficient and environmental friendly and growing technique recently. The mechanism of this process is based on the activity of Fe<sup>2+</sup> and Fe<sup>3+</sup> ions in the system initiating the peroxide radicals for further oxidation step to the organic molecules (Perez *et al.*, 2002a,b; Al-Kdasi *et al.*, 2004). In Fenton reaction, hydroxyl radicals ·OH are produced by interaction of H<sub>2</sub>O<sub>2</sub> with ferrous salts according to Eq. 1.



Fe<sup>3+</sup> can react with H<sub>2</sub>O<sub>2</sub> in the Fenton-like reaction (Eq. 2-4), regenerating Fe<sup>2+</sup> and thus supporting the Fenton process (Perez *et al.*, 2002a, b).



In conjunction with  $\text{Fe}^{3+}/\text{Fe}^{2+}$ , the irradiation of the system with UV source in presence of  $\text{TiO}_2$  results in significant enhancement of the oxidation rate. When the system is irradiated with UV illumination, the degradation rate of the organic pollutants by Fenton and Fenton-like reaction can increase through the involvement of high valence iron intermediates, responsible for the direct attack on organic matter (Perez *et al.*, 2002a, b). The absorption of visible light by the complex formed between  $\text{Fe}^{3+}$  and  $\text{H}_2\text{O}_2$  could be the cause of these intermediates.

On the other hand, the combination of  $\text{Fe}^{3+}/\text{Fe}^{2+}$  with  $\text{TiO}_2$  aids in enhancement in the generation of OH radical, resulting in the increase of the contaminant degradation. The combination of  $\text{Fe}^{3+}/\text{Fe}^{2+}$  with  $\text{TiO}_2$  for photocatalytic degradation of organic molecules has been reported earlier (Sonawane *et al.*, 2004; Zhu *et al.*, 2007). Although, this process promises as an effective technique for pollutant oxidation, it faces several process and economic downturns due to the high cost of filtration and recovery of expensive  $\text{TiO}_2$  particles. Furthermore, while using the bulk amount of  $\text{TiO}_2$ , results in particle aggregation thereby reducing its total surface exposure to UV radiation. On the similar lines application of Fe ions in the homogeneous phase, pose a major problem in the treatment of Fe containing sludge produced further downstream in the waste treatment plant. In-order to counter these issues, it is proposed to immobilize both  $\text{TiO}_2$  and Fe Ion on inorganic matrix to reduce the loss and enhance the photocatalytic activity (Li *et al.*, 2006; Noorjahan *et al.*, 2006; Antoniou and Dionysioa, 2007).

Compared to various other techniques of titania immobilization, the synthesis of titania pillared clays demonstrate its advantage in several aspects. Clays are abundant material and pillared clays are generally stable in heterogeneous chemical condition. Additionally, some titania pillared clays produce pore openings of about 1 nm or even larger (Miao *et al.*, 2006; Pichat *et al.*, 2005; Rezala *et al.*, 2009). This provides higher specific surface area to serve as photocatalyst via heterogeneous mechanism. As other metal oxide pillarization of clays, the titania pillared clays having cationic sites which are possible to be replaced by other cations such as iron (III).

We report in this study the synthesis of Fe(III) exchanged titania pillared clays and its property as photocatalyst. Natural montmorillonite was pillared using titanium oxide chloride precursor. The photocatalytic activity of iron exchanged  $\text{TiO}_2$ -Montmorillonite (Fe/TiM) was investigated using the methyl orange (MeO) photooxidation by Photo-Fenton like system with hydrogen peroxide ( $\text{H}_2\text{O}_2$ ) as an oxidant. Different parameters were also examined.

## MATERIALS AND METHODS

### Synthesis of iron exchanged titanium montmorillonite:

The montmorillonite (with CEC of 68-86 mEq/100 g) was supplied by PT. Tunas Inti Makmur Semarang, Indonesia. The titanium oxide pillared montmorillonite was prepared by using titanium oxide chloride ( $\text{TiOCl}_2$ , supplied by E.Merck) as pillaring agent. The pillaring solution was prepared by dilution of  $\text{TiOCl}_2$  solution with HCl 0.1 M under vigorously stirring to get transparent solution. Then it was added to a suspension of the montmorillonite within the ratio of Ti equal to 5 mmol  $\text{g}^{-1}$  clay. The mixture was stirred for 4 h. The resulting product was separated by filtration, followed by washing several times with deionized water to neutralize and remove Cl ions, then dried in the oven at 70°C. The Titanium intercalated clay was calcined in nitrogen flow at the temperature of 400°C for 4 h to obtain the pillared material. The sample was assigned as TiM.

The iron(III)-exchanged TiM (Fe/TiM) was prepared by mixing TiM with iron (III) ammonium sulphate solution, at a molar ratio of Fe(III) to CEC of TIM 0.25 under refluxing for 6 h. The solid was filtered and washed with deionized water then dried at 60°C. The ion-exchange process was replicated for three times.

**Characterization technique:** The diffraction patterns to identify the phase of natural montmorillonite, TiM and Fe/TiM catalysts were recorded with Shimadzu X6000 X-ray diffractometer using Cu  $\text{K}\alpha$  radiation, with accelerating voltage of 40 kV, current 30 mA and scanned at the  $2\theta$  from 5 to 70°. The optical absorption of the photocatalyst was determined using UV-vis Diffuse reflectance spectroscopy measurements conducted with JASCO V-760. Surface area and pore size was determined by nitrogen adsorption-desorption, measured using Gas sorption analyzer NOVA 1200e. The content of Ti and Fe present in the sample was analyzed by X-ray fluorescence spectrophotometry.

**Photocatalytic activity test:** The methyl orange dye has a molecular weight of 327.33  $\text{g mol}^{-1}$  and chemical formula of  $\text{C}_{14}\text{H}_{14}\text{N}_3\text{SO}_3\text{Na}$ . It was used as received and its structure is shown in Fig. 1.

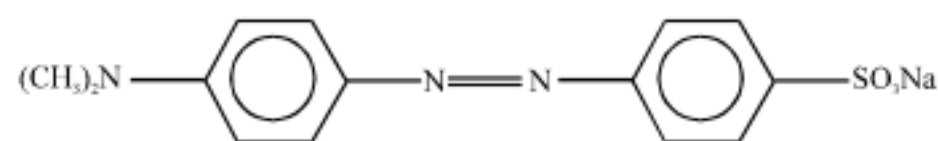


Fig. 1: Molecular structure of MeO

The photocatalytic activity of Fe/TiM was examined in the photo-assisted degradation of methyl orange in the presence of H<sub>2</sub>O<sub>2</sub> and UV light at optimized conditions. The choice of methyl orange (MeO) as model pollutant lies in the fact that it is a typical non-biodegradable anionic azo-dye. The photo reactor consisted of a rectangular box, fitted with one UVC light tube (Philips, 10W 254 nm) and one UVB light tube (10W 356 nm) placed hang on top. A fixed amount of catalyst and oxidant was added to 500 mL of dye solution under constant stirring. The experiments were carried out at 20°C. The MeO degradation efficiency was evaluated by percentage of degraded MeO measured by UV-visible spectrophotometry (Hitachi U 2010) at the wavelength of 465 nm.

**RESULTS AND DISCUSSION**

**Catalyst characterization:** Figure 2 shows the N<sub>2</sub> adsorption-desorption isotherms of TiM and Fe/TiM. The natural montmorillonite was presented for comparison. Significant change of the N<sub>2</sub> adsorption isotherm was observed for TiM and Fe/TiM, with higher amount of adsorbed nitrogen molecules at lower relative pressures compared to the starting montmorillonite. This improvement was due to the presence of the pillaring species in the interlayer gallery.

For TiM and Fe/TiM, at high p/po value, isotherm correspond to the type II class according to the Brunauer, Deming, Deming and Teller classification (BDDT), which is characteristic of systems with a large pore size range. This indicates the improvement of adsorption capacity and in agreement with the specific surface area and pore volume data as shown in Table 1.

The presence of hysteresis loops indicates mesoporosity in both materials. Table 1 summarizes the textural properties of the prepared pillared clays. The deduced surface area from the BET equation was higher for Fe/Ti-M and TiM compared to the starting clay. These data are in agreement with was reported by Rezala *et al.* (2009) in which the titania pillarization increase the specific surface area and pore volume. However, although the isotherm suggest the mesoporous formation in TiM and Fe/TiM, the average pore diameter was in the range of microporous materials (Table 1). The possible reason for this fact is come from the formation of ‘‘house of cards’’ structure in pillared material as the result of the attraction between negatively charged basal surfaces and positively charged crystal edges. Highly acid environment of titanium ions in precursor solution potentially damage

Table 1: Physical parameter of materials

Parameters	Natural montmorillonite	TiM	Fe/TiM
Specific Surface area (m <sup>2</sup> g <sup>-1</sup> )	45,68	127.06	120.09
Pore Volume (10 <sup>-3</sup> cc g <sup>-1</sup> )	0.037	156.000	152.000
Pore Radius (Å)	16.436	15.193	15.21
Ti content (%w/w)	-	10.96	10.95
Fe content (%w/w)	0.65	0.63	2.48

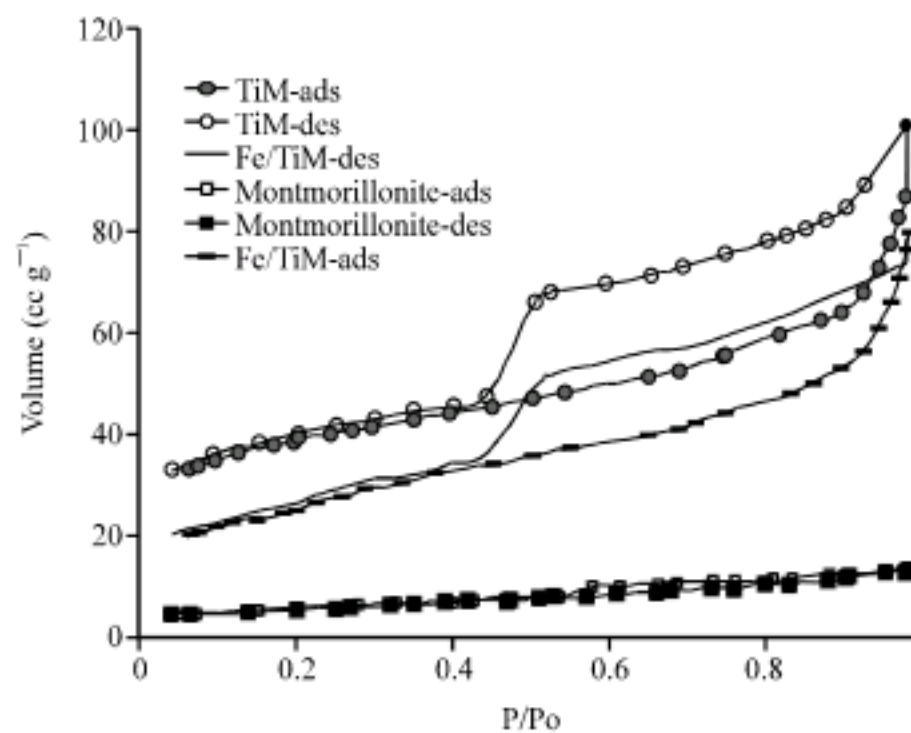


Fig. 2: Nitrogen Adsorption-desorption porofile of materials (ads: adsorption, des:desorption)

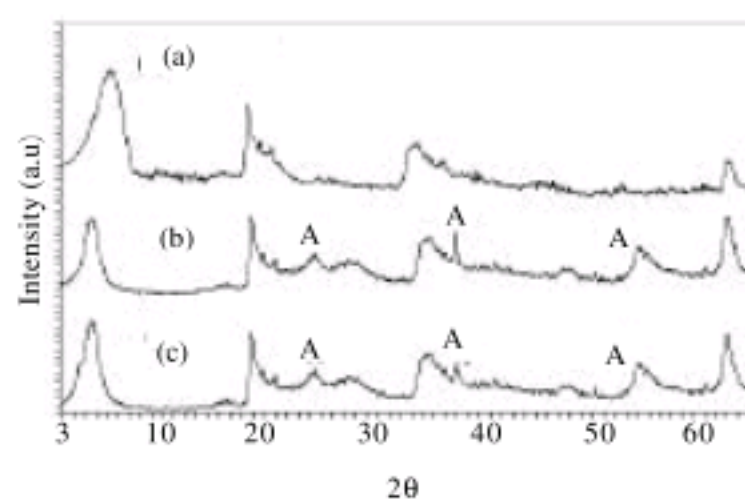


Fig. 3: XRD pattern of (a) natural montmorillonite (b) TiM (c) Fe/TiM (A is indication for anatase phase)

to the clay structure (Yuana *et al.*, 2006). The slight variation in the textural properties of Ti-M and Fe/Ti-M could be related to the lower content of Fe/Ti-M in iron. (Table 1).

Powder XRD patterns of the different catalysts are presented in Fig. 3. The position of the first reflection shifted to lower angle, due to the expansion of the interlayer spacing by the pillaring species from 0.96 nm to 3.2 nm for Ti-M. The addition of Fe ions did not affect the interlayer spacing and it remained unchanged for Fe/Ti-M. Additional reflections for Ti-M and Fe/Ti-M were observed in the region of 2θ angle at 25.1°, 37.7° and 53.8°. They were assigned to the (101), (004) and (105) reflections of tetragonal titania in anatase phase. In

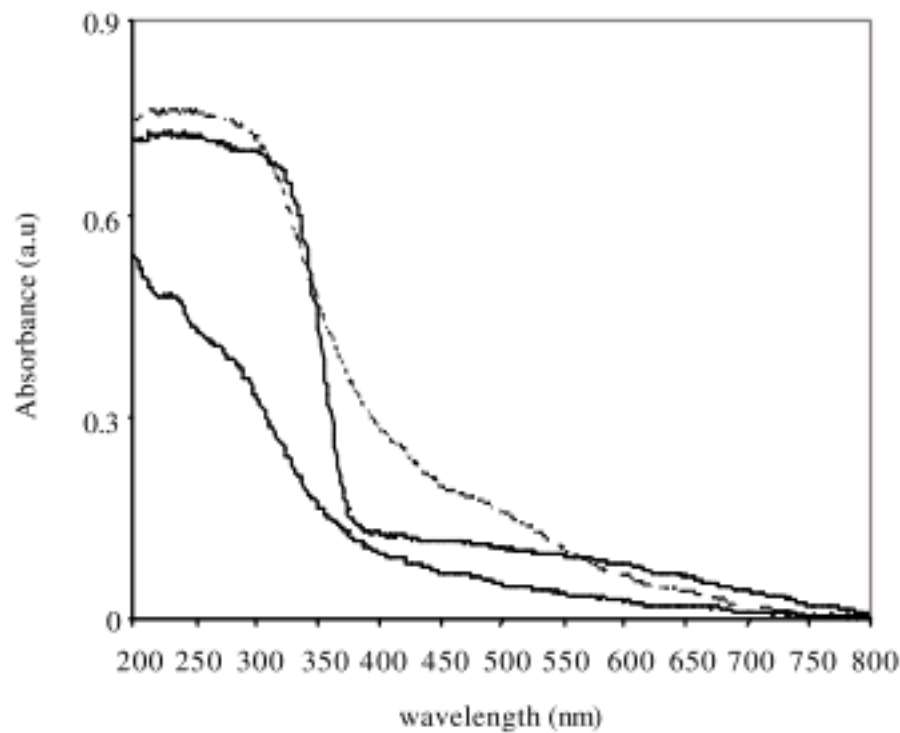


Fig. 4: DRUV-visible spectra of materials

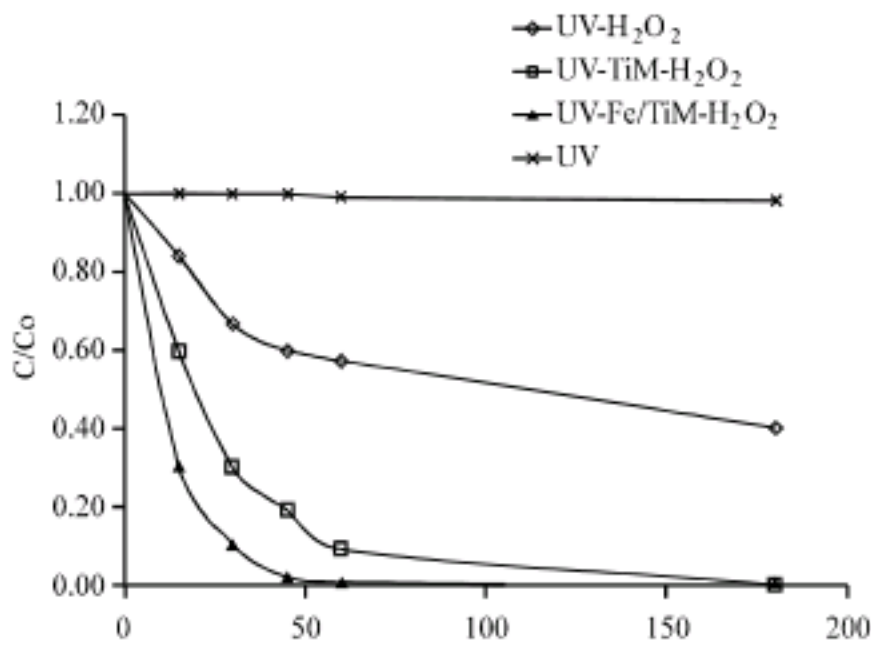


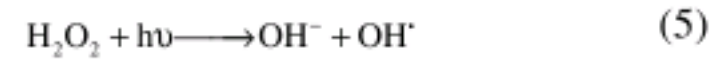
Fig. 5: Kinetics of MeO decolorization by varied treatments (Condition: [MeO] =  $5 \times 10^{-4}$  M, [H<sub>2</sub>O<sub>2</sub>] =  $2 \times 10^{-5}$  M)

Fe/Ti-M catalysts, It was difficult to detect iron oxide phase and could indicate that the iron is available in its ionic form, as requested in the photo-Fenton mechanism.

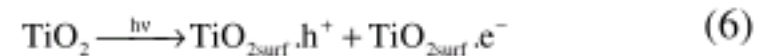
The UV-vis diffuse reflectance absorption spectrum of Ti-M exhibits broad absorbance band at about 340 nm, characteristic of titanium oxide species (Fig. 4) The presence of Fe ions in Ti-M resulted in the red shift of the band gap as well as an increase in absorption intensity (Fig. 4). This shift may be correlated to the interaction between Fe<sup>3+</sup> and H<sub>2</sub>O which lies at visible region.

**Photoactivity test:** Preliminary experiments conducted to analyze the photocatalytic activity of Fe/TiM shows a higher activity as compared to TiM. As shown in Fig. 5, MeO shows negligible degradation under the influence of UV radiation however, the reaction is almost 60% complete in the presence of H<sub>2</sub>O<sub>2</sub> and UV. The oxidation of MeO under UV-H<sub>2</sub>O<sub>2</sub> system is due to the formation of

active hydroxyl radicals. Under the influence of UV radiation (approx~250 nm), peroxide is known to undergo a direct photo-dissociation to generate hydroxyl radicals following reaction (Eq. 5) which are known to have a high oxidation potential of 2.6 eV (Bauer and Fallmann, 1997).



Further test, in the presence of TiM and Fe/TiM shows complete reaction in much shorter time, indicating the additional effect of the presence of TiO<sub>2</sub> and Fe ions. The presence of Fe<sup>3+</sup> ion in the system can be assumed to play two important roles to enhance the rate of reaction. Firstly, it would act as a possible quencher of the available electrons generated on the TiO<sub>2</sub> surface from the absorption of the UV radiation, which will then prevent the recombination of the electron-hole pair on the photo catalyst surface, as per the following reactions (Eq. 6, 7).



Alternatively, the available Fe<sup>2+</sup> and Fe<sup>3+</sup> would individually under modified Fenton reaction under the presence of H<sub>2</sub>O<sub>2</sub> to produce active hydroxyl radical for the degradation of MeO. Overall, the combination of TiO<sub>2</sub> and Fe under the influence of light and H<sub>2</sub>O<sub>2</sub>, results in series of reaction as shown in Fig. 5 resulting in faster degradation of MeO.

The reaction mechanism of MeO oxidation step has been well correlated by the Langmuir-Hinshelwood kinetics, wherein the MeO molecule is initially adsorbed on the catalyst surface and is further reacted by the first order reaction rate from the available active hydroxyl radicals.

The kinetic model is given as Eq. 8.

$$\frac{dC_{\text{MeO}}}{dt} = \frac{kKC_{\text{MeO}}}{1 + KC_{\text{MeO}}} \quad (8)$$

where, k is the rate constant and the K is the equilibrium adsorption constant.

The base constants can be estimated by plotting data for reaction rate at different initial concentrations of MeO. An equivalent expression for the Langmuir-Hinshelwood kinetics is shown in Eq. 9.

$$\frac{1}{R_0} = \frac{1}{k} + \frac{1}{kK[C_{\text{MeO}}]_0} \quad (9)$$

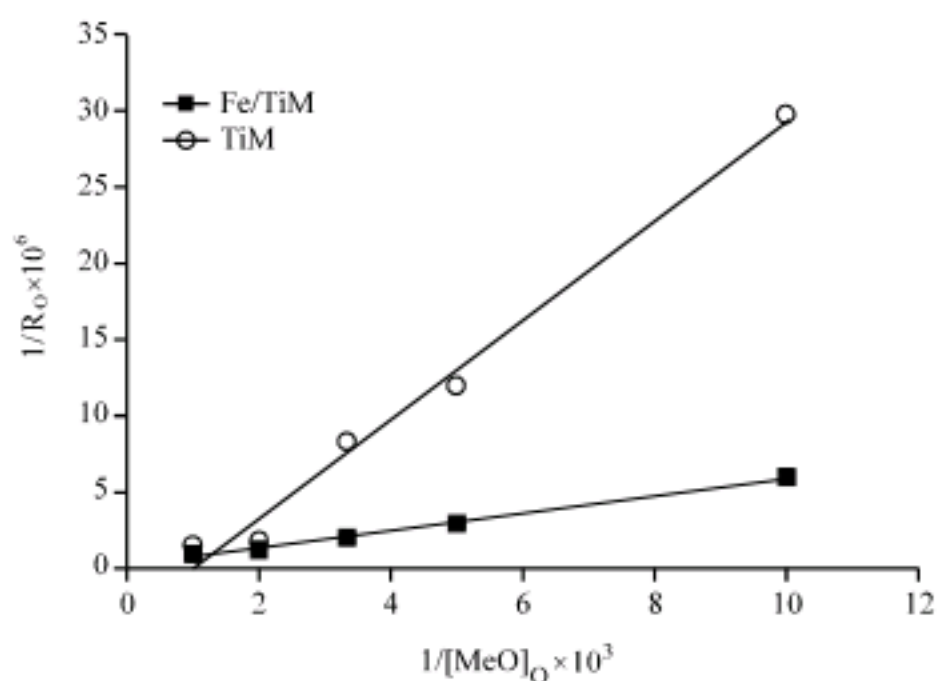


Fig. 6: Langmuir-Hinshelwood Plot of MeO decolorization by TiM and Fe/TiM catalyst (Condition catalyst = 0.5% w/w,  $[H_2O_2] = 2 \times 10^{-5} M$ )

From the intercept and slope values of  $1/\text{rate}$  plotted against  $1/[MeO]_0$ , the constants,  $k$  and  $K$  can be obtained from the intercept and slope. The plot is shown in Fig. 6.

Due to the Langmuir-Hinshelwood plot in Fig. 6, the rate constant ' $k$ ' of TiM and Fe/TiM are observed to be  $1.67 \times 10^{-7} \text{ mol L}^{-1}$  and  $8.84 \times 10^{-7} \text{ mol L}^{-1}$ , respectively. The adsorption constant,  $K$  for each are  $307.82 \text{ L mol}^{-1}$  and  $328.29 \text{ L mol}^{-1}$ . Data used for this calculation was obtained by measuring the initial reaction rate with different initial concentrations of MeO, from  $1.0 \times 10^{-4} \text{ mol L}^{-1}$  to  $1 \times 10^{-4} \text{ mol L}^{-1}$ . From the correlated constants it can be observed that the dye adsorption remained effectively similar for TiM and Fe/TiM, whereas the rate of reaction increased several folds. This observation is in accordance with the fact that TiM and Fe/TiM had similar surface area resulting in similar adsorption whereas the presence of Fe ions subsequently increased the reaction rate due to additional formation of hydroxyl radicals.

Efficiency of decolorization in this research is higher compared with the previous results of methyl orange decolorization using  $TiO_2$  catalyzed photodegradation system reported by Razed and El-Amin (2007) in which degradation percentage is around 23.57-47.02% at the MeO concentration range of  $10^{-8}$ - $10^{-5} M$ . In addition, efficiency in this study is also found slightly higher compared to was reported by Guettaï and Ait Ammar (2005) in similar system used by Razed and El-Amin (2007). Although, there was possible different light sources of both experiments and what conducted in this research, interpretation of the degradation kinetics consider the synergistic effect between both

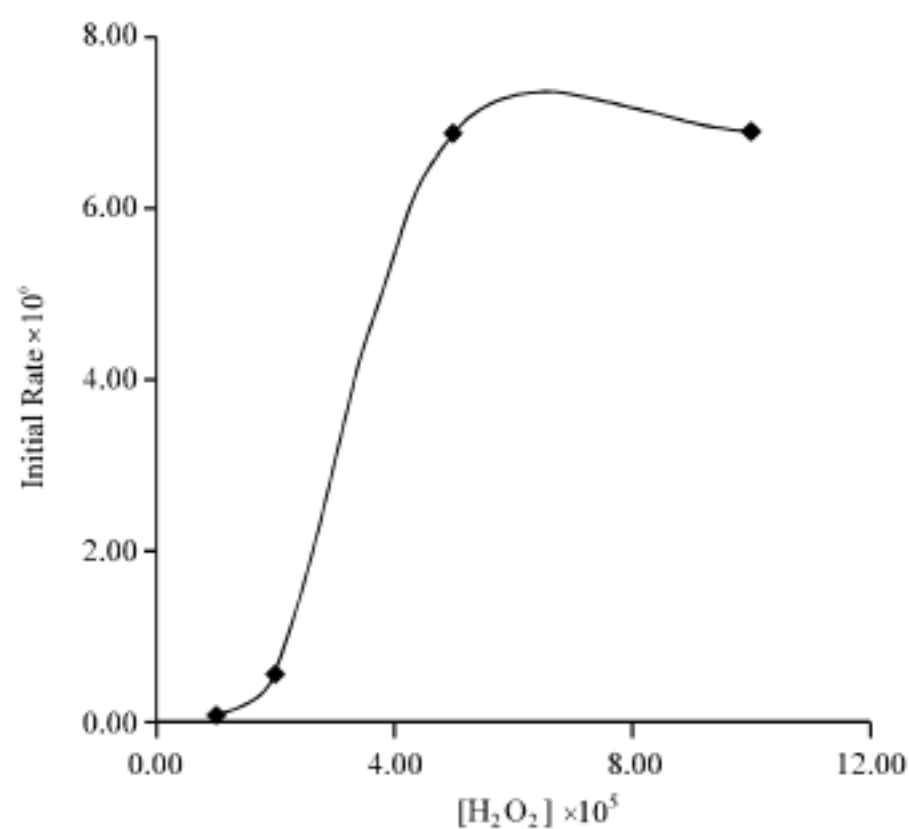


Fig. 7: Effect of  $H_2O_2$  concentration to the Initial rate

photocatalytic and photo-Fenton mechanism within UV-Fe/TiM- $H_2O_2$  system as new mechanism in the photodegradation. This result shows the success of catalyst modification aimed to combine by both  $TiO_2$  photocatalytic mechanism and UV- $Fe^{3+}$ - $H_2O_2$  photo-Fenton mechanism simultaneously within the system.

#### Effect of reaction parameter

**Effect of  $H_2O_2$ :** The amount of oxidant present in the sample determines the rate of generation of hydroxyl radical responsible for dye discoloration. To evaluate the effect of  $H_2O_2$  on the degradation rate, studied were conducted at different amount of  $H_2O_2$  ranging from  $1 \times 10^{-5} M$ , to  $10^{-4}$ . Figure 7 shows the effect of oxidant amount on the initial rate of reaction.

The rate profile suggests that the rate of MeO oxidation increased significantly with the increase in the concentration of oxidant until reaching a maximum of around  $4 \times 10^5 M$ . within the range of 2 to  $4 \times 10^{-5} M$ . However, a slight increase was observed at higher concentrations. This fact may be due to the hydroxyl radical scavenging effect of  $H_2O_2$  and recombination of hydroxyl radicals by  $H_2O_2$  at high concentration. This effect was also observed by Li *et al.* (2006) in the Photo-Fenton degradation of azo dye by using iron pillared bentonite.

**Effect of catalyst dosage:** Changing the amount of catalyst in the reaction system, affects the reaction rate by providing additional surface for the adsorption as well as generating oxidative valence band holes and electrons. To determine the effect of catalyst loading on the reaction rate, several experiments were conducted for catalyst

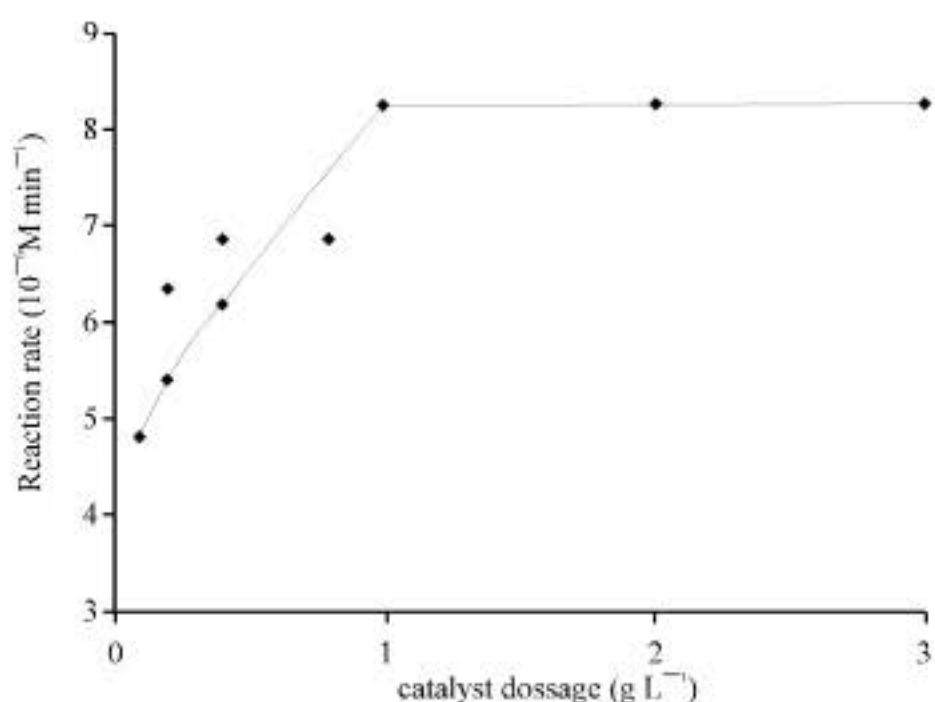


Fig. 8: Effect of catalyst dosage to reaction rate

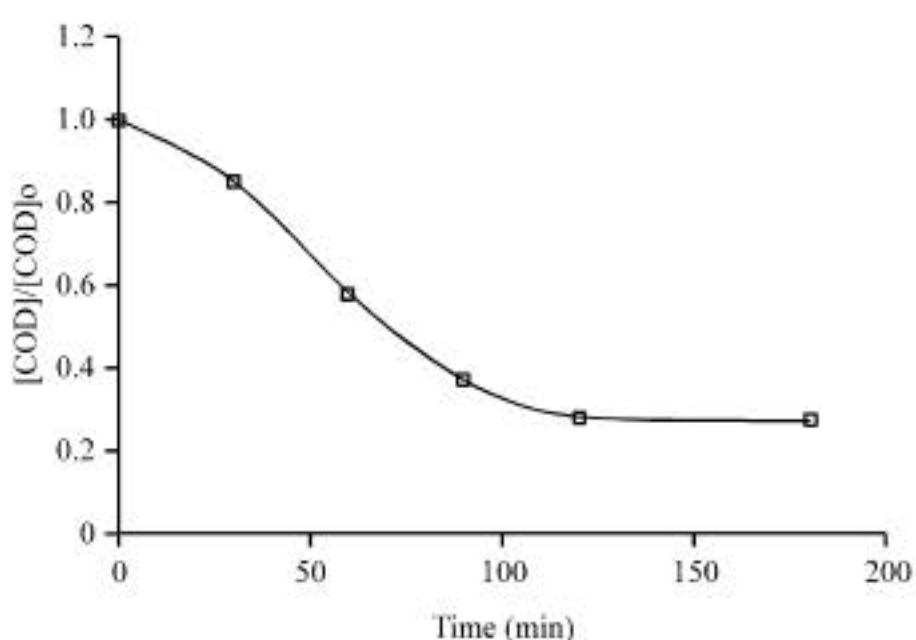


Fig. 9: COD removal as function of reaction time (Condition : [MeO] = 5×10<sup>-4</sup> M, [H<sub>2</sub>O<sub>2</sub>] = 2×10<sup>-5</sup> M)

amounts from 0.1 to 3 g L<sup>-1</sup>. The curve representing effect of catalyst dosage to the reaction rate is shown in Fig. 8.

The addition of catalyst results in increasing the degradation rate until a maximum amount of 2 g L<sup>-1</sup> is reached, further to which the degradation rate remains almost similar. Increasing the amount of catalyst provides an additional TiO<sub>2</sub> and Fe ions which aids in faster rate of reaction, however the incremental benefit of increased concentration TiO<sub>2</sub> and Fe ions is offset by the reduced UV transmission in the solution resulting from the hazy solution obtained by the excess addition of catalyst. This causes a decrease in the amount of energy being received by the particles. Earlier work done on photocatalytic reaction using titanium dioxide catalyst by Baran *et al.* (2008) and Chiou *et al.* (2008) suggested that the rate of reaction decreases due to excess addition of catalyst resulting from reduced light transmission, however in the current study, the presence of Fe catalyst still continues to oxidizes the dye in spite of reduction in the UV transmission and hence the reaction rate is prevented from decreasing.

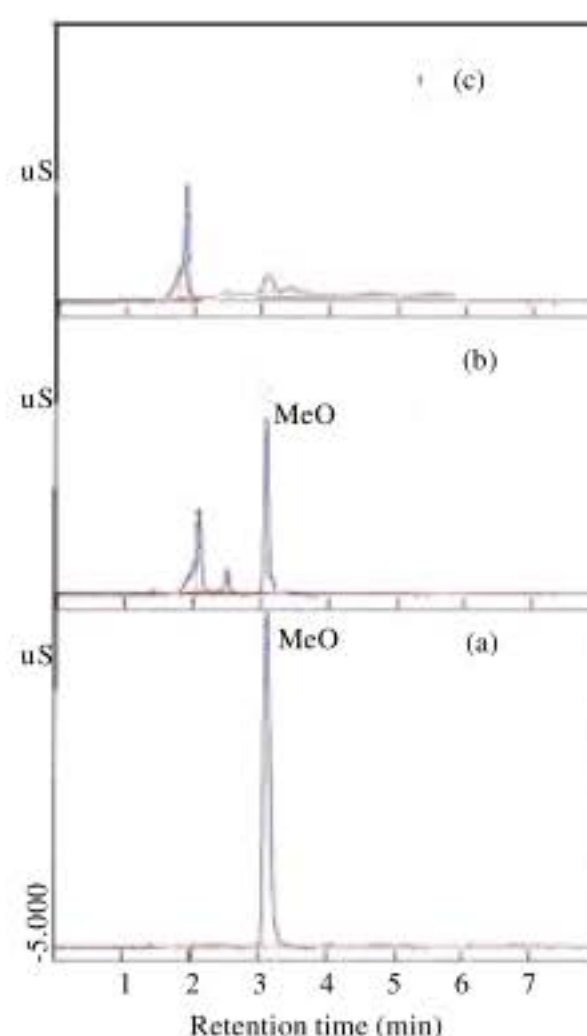


Fig. 10: Chromatogram of MeO solution (a) initial (b) after 1 h treatment and (c) after 3 h treatment

**Extent of mineralization of dye:** As other dye photodegradation, complete oxidation process will produce CO<sub>2</sub>, H<sub>2</sub>O and NO<sub>2</sub> as released gas from solution. Chemical Oxygen Demand (COD) value can be useful measurement to monitor the kinetic of dye degradation in that the higher COD value will describe the organic compound presence in treated solution. The COD value of MeO solution treated with UV-Fe/TiM-H<sub>2</sub>O<sub>2</sub> system as function of time was measured and the result is shown in Fig. 9.

In contrast to complete dye discoloration obtained within 1 h, the extent of COD removal was just 40%. Further analysis showed almost 80% removal in 3 h of reaction time. The different in reduction of values correlate with the mechanism of MeO photooxidation in the system. During the reaction periode, there was incomplete oxidation process to MeO and left chemical intermediates in the water contribute to COD value.

The presence of intermediates resulting from the degradation of MeO, was observed from the HPLC analysis with the chromatograms shown in Fig. 10. It can observed that stable intermediates such as sulphonic acids are formed due to the oxidation of MeO, which are hard to oxidize quickly and hence results in slower reduction in the amount of COD.

**Catalyst reusability:** One important issue in Fe/TiM application is the immobilized iron (III) in order to minimize

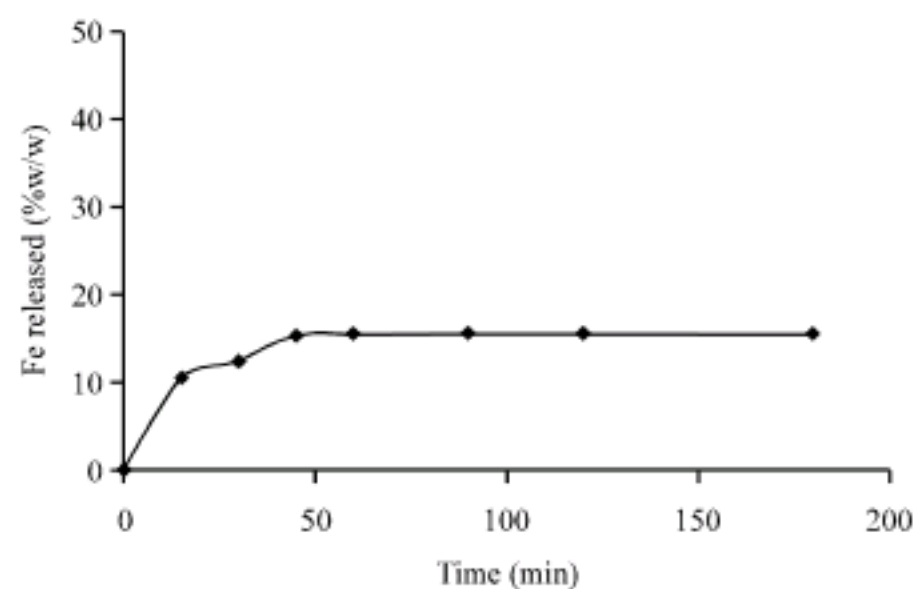


Fig. 11: Fe released in solution as function of time (Condition:  $[MeO] = 5 \times 10^{-4} M$ ,  $[H_2O_2] = 2 \times 10^{-5} M$ )

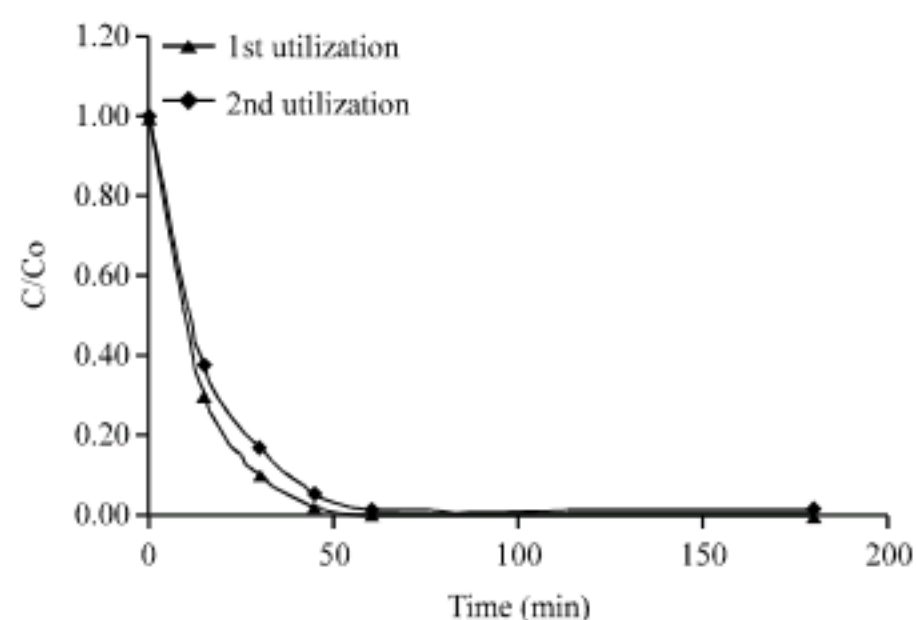


Fig. 12: Comparison of kinetic degradation of MeO by using Fe/TiM in first and second utilization (Condition:  $[MeO] = 5 \times 10^{-4} M$ ,  $[H_2O_2] = 2 \times 10^{-5} M$ )

the Fe leaching in water and its reuse. Evaluation on catalyst reusability was engaged by analyzing Fe released in treated MeO solution and study the used catalyst in the same MeO photodegradation reaction. Figure 11 shows the percentage of Fe leached in solution compared to the Fe content in Fe/TiM as function of time.

As shown in Fig. 11, Fe was found in solution in small portion as dissolved ion and it reach maximum concentration in 1 h. The released Fe seems to be constant at additional time. The leached Fe indicate the presence of weakly bonded Fe in TiM which was easily desorbed to the solution. It may caused by incompletely washing during Fe immobilization and left the excess Fe deposited on TiM surface. Furthermore, the MeO degradation by using pre-used catalyst compared to the fresh catalyst was evaluated. The kinetic curves is presented in Fig. 12 .

According to the kinetic curve in Fig. 12, it is found that slight abatement of degradation rate in second

utilization of Fe/TiM compared to the fresh Fe/TiM. The meaningful differences of reaction rate show at the range of 1 h reaction time, moreover MeO reduction remained constant. The activity in second utilization was also still higher compared to the TiM activity (Fig. 5), suggesting that however there was Fe released in first utilization, Fe/TiM catalyst still active enough compared to the fresh one.

## CONCLUSION

The iron exchanged titanium pillared montmorillonite has been successfully synthesized and characterized. The photocatalytic activity of the synthesized material was examined by the oxidation of MeO under the presence of hydrogen peroxide. The study suggests that combining the Fenton and photocatalytic reaction helps in significantly enhancing the rate of reaction. Furthermore, immobilizing the  $TiO_2$  and Fe ion on a single support helps in reducing the loss of the catalyst into the discharged water. The reaction was found to be significantly affected by the amount of  $H_2O_2$  as oxidant and catalyst dosage. The decolorization rate of MeO by the prepared material was observed to be quite increase and obey Langmuir-Hinshelwood kinetics model.

## ACKNOWLEDGMENTS

The authors would like to express sincerely gratitude to Chemistry Dept., Islamic University of Indonesia for the financial and technical support to accommodate this research.

## REFERENCES

- Al-Kdasi, A., A. Idris, K. Saed and C.T. Guan, 2004. Treatment of textile wastewater by advanced oxidation processes: A-review. *Global Nest: Int. J.*, 6: 222-230.
- Antoniou, M.G. and D.D. Dionysiou, 2007. Application of immobilized titanium dioxide photocatalysts for the degradation of creatinine and phenol, model organic contaminants found in NASA's spacecrafts wastewater streams. *Catalysis Today*, 124: 215-223.
- Baran, W., E. Adamek and A. Makowski, 2008. The influence of selected parameters on the photocatalytic degradation of azo-dyes in the presence of  $TiO_2$  aqueous suspension. *Chem. Eng. J.*, 145: 242-248.
- Bauer and Fallmann, H., 1997. The photo-fenton oxidation-a cheap and efficient wastewater treatment method. *Res. Chem. Intermediates*, 23: 341-354.



- Chiou, C., C. Wu and R. Juang, 2008. Influence of operating parameters on photocatalytic degradation of phenol in UV/TiO<sub>2</sub> process. *Chem. Eng. J.*, 139: 322-329.
- Guettaï, H. and H. Ait Ammar, 2005. Photocatalytic oxidation of methyl orange in the presence of titanium dioxide in aqueous suspension. Part I: Parametric study. *Desalination*, 185: 427-437.
- Li, Y., Y. Lu and X. Zhu, 2006. Photo-Fenton discoloration of the azo dye X-3B over pillared bentonites containing iron. *J. Hazard. Mater.*, 32: 196-201.
- Miao, S., S. Liu, B. Han, J. Zhang, X. Yu, J. Du and A. Sun, 2006. Synthesis and characterization of TiO<sub>2</sub>-montmorillonite nanocomposites and their application for removal of methylene blue. *J. Mater. Chem.*, 16: 579-584.
- Noorjahan, M., D. Kumari, V. Subrahmanyam and L. Panda, 2006. Immobilized Fe(III)-HY: An efficient and stable photo-Fenton catalyst. *Applied Catalysis B*, 57: 291-298.
- Perez, M., F. Torrades, X. Domenech and J. Peral, 2002a. Fenton and photo-fenton oxidation of textile effluents, *Water Res*, 36: 2703-2710.
- Perez, M., F. Torrades, J.A. Gracia-Hortal, X. Domènech and J. Peral, 2002b. Removal of organic contaminants in paper pulp treatment effluents under Fenton and photo-Fenton conditions. *Applied Catalysis B: Environ.*, 36: 63-74.
- Pichat, P., H. Khalaf, D. Tabet, M. Houari and M. Saidi, 2005. Ti-montmorillonite as photocatalyst to remove 4-chlorophenol in water and methanol in air. *Environ. Chem. Lett.*, 2: 191-194.
- Razed, M.N. and A.A. El-Amin, 2007. Photocatalytic degradation of methyl orange in aqueous TiO<sub>2</sub> under different solar irradiation sources. *Int. J. Phys. Sci.*, 2: 073-081.
- Rezala, H., H. Khalaf, J. Valverde, A. Romero, A. Molinari and A. Maldotti, 2009. Photocatalysis with Ti-pillared clays for the oxofunctionalization of alkylaromatics by O<sub>2</sub>. *Applied Catalysis A: Gen.*, 352: 234-242.
- Sonawane, R.S., B.B. Kale and K. Dongare, 2004. Preparation and photocatalytic activity of Fe-TiO<sub>2</sub> thin films prepared by sol-gel dip coating. *Mater. Chem. Phys.*, 85: 52-57.
- Yuana, P., X. Yina, H. Hea, D. Yanga, L. Wangc and J. Zhua, 2006. Investigation on the delaminated-pillared structure of TiO<sub>2</sub>-PILC synthesized by TiCl<sub>4</sub> hydrolysis method. *Microporous Mesoporous Mater.*, 93: 240-247.
- Zhu, J., J. Ren, Y. Huo, Z. Bian and L. Hexing, 2007. Nanocrystalline Fe/TiO<sub>2</sub> visible photocatalyst with a mesoporous structure prepared via a nonhydrolytic sol-gel route. *J. Phys. Chem. C*, 111: 18965-18969.